ACOUSTIC EMISSION SOURCE LOCALIZATION USING DEEP TRANSFER LEARNING AND FINITE ELEMENT MODELING–BASED KNOWLEDGE TRANSFER

XUHUI HUANG*, OBAID ELSHAFIEY*, KARIM FARZIA†, LALITA UDPA*, MING HAN*, AND YIMING DENG*‡

ABSTRACT

This paper presents a novel data-driven approach to localize two types of acoustic emission sources in an aluminum plate, namely a Hsu-Nielsen source, which simulates a crack-like source, and steel ball impacts of varying diameters acting as the impact source. While deep neural networks have shown promise in previous studies, achieving high accuracy requires a large amount of training data, which may not always be feasible. To address this challenge, we investigated the applicability of transfer learning to address the issue of limited training data. Our approach involves transferring knowledge learned from numerical modeling to the experimental domain to localize nine different source locations. In the process, we evaluated six deep learning architectures using tenfold cross-validation and demonstrated the potential of transfer learning for efficient acoustic emission source localization, even with limited experimental data. This study contributes to the growing demand for running deep learning models with limited capacity and training time and highlights the promise of transfer learning methods such as fine-tuning pretrained models on large semi-related datasets.

KEYWORDS: acoustic emission, deep neural network, finite element modeling, transfer learning, fiber optics, source localization

Introduction

Acoustic emission source localization is crucial in structural health monitoring (SHM) and proactive maintenance of metallic structures. The constraints in deploying acoustic emission testing (AE) sensor arrays in real-world structures necessitate a shift toward intelligent, automated single-sensor approaches. Holford et al. (2001) pioneered the application of AE for damage location in steel bridges, establishing its importance in SHM. Ebrahimkhanlou and Salamone (2017) further examined acoustic source localization and its significance in determining the origin of acoustic emission waves and assessing damage severity. Cheng et al. (2021) developed an acoustic emission source localization method using Lamb wave propagation simulation and artificial neural networks, proving effective in I-shaped steel girder inspections. Ai et al. (2021) studied source localization on large-scale canisters used for nuclear fuel storage, addressing the need for optimal AE sensor deployment. Ciampa and Meo (2010) proposed an approach using wavelet analysis and a Newton-based optimization technique for acoustic emission source localization and velocity determination, contributing to the broader understanding of acoustic emission wave propagation and source detection.

Significant progress has been achieved in acoustic emission source localization through the application of deep learning, demonstrating its promise in localizing acoustic emission signals (LeCun et al. 2015). Ebrahimkhanlou and Salamone (2018) proposed a deep learning approach for localizing acoustic emission sources using a single sensor in plate-like structures. This was further advanced by Ebrahimkhanlou et al. (2019), who introduced a deep learning–based framework for localizing and characterizing acoustic emission sources in metallic panels using only one sensor. Garrett et al. (2022) utilized artificial intelligence for estimating fatigue crack length from acoustic emission waves, a significant step forward in damage localization and quantification. Despite the challenge of false positives, the fusion of artificial intelligence and AE holds promising opportunities for enhancing SHM (Verstrynge et al. 2021; Hassan et al. 2021).

A key challenge in using supervised learning algorithms for acoustic emission source localization is the difficulty in accessing labeled acoustic emission signals for existing structures. Transfer learning is a strategy that assists the supervised learning task when available training data is limited

* Department of Electrical and Computer Engineering, Michigan State University, East Lansing, MI
† Nikon Inc., 9453 Innovation Dr., Manassas, VA
‡ Corresponding author: dengyimi@egr.msu.edu

Materials Evaluation 81 (7): 71–84
https://doi.org/10.32548/2023.me-04348

(Agarwal et al. 2021). Various studies have demonstrated the value of transfer learning in enhancing neural networks for acoustic emission source localization and SHM, such as Chen et al. (2021), who proposed an acoustic-homologous transfer learning approach for rail condition evaluation, and Hasan et al. (2019), who utilized transfer learning for reliable bearing fault diagnosis under variable speed conditions.

Deep learning and transfer learning methods have shown great potential in improving acoustic emission source localization efficiency (Sun 2020; Bengio 2012). Ismail-Fawaz et al. (2022) presented a deep learning approach for time series classification using hand-crafted convolution filters, further enhancing AE capabilities. Ismail Fawaz et al. (2018) explored transfer learning for time series classification, while Zhang et al. (2017) studied the learnability of fully connected neural networks. Weiss et al. (2016) provided a survey of transfer learning, and Bengio (2012) emphasized the importance of deep learning representations for unsupervised and transfer learning. Though significant advancements have been made in applying deep learning and transfer learning to acoustic emission source localization, continued development and optimization of these methodologies are essential for addressing inherent challenges and maximizing their potential in SHM (Bengio 2012; Sun 2020).

In this study, our principal innovation lies in the successful implementation of transfer learning through the pretraining of six deep learning models on a large simulated acoustic emission dataset. This enabled the localization of acoustic emission sources using a single sensor. We pretrained convolutional neural network (CNN), fully convolutional neural network (FCNN), Encoder, ResNet, Inception, and Multi-layer Perceptron (MLP) models using data from finite element method (FEM) simulations of acoustic emission impulses. Through transfer learning, we fine-tuned the pretrained models on the experimental dataset, improving their performance while reducing the number of experiments needed. Our results show that the pretrained models generalized well to variations in acoustic emission signals and could be applied to different model architectures and datasets. Overall, our research highlights the potential of deep learning techniques, particularly transfer learning, for improving the accuracy and efficiency of acoustic emission source localization. These findings can significantly benefit the development of reliable and cost-effective SHM strategies and are readily applicable to other nondestructive evaluation problems.

This paper is organized into four main sections. The first section provides an overview of the laboratory experiments conducted utilizing pencil lead break (PLB) and impact tests at nine distinct positions. In the next section, to aid understanding, data visualization is furnished through raw waveform plots of both simulated and real-life experimental data derived from impact and PLB testing. Additionally, a 2D t-SNE plot is provided to better illustrate the clustering structure of signals originating from nine distinct locations or classes. The third section introduces six distinct deep learning models, including our own, which were designed through the iterative fine-tuning of layers with unique training parameters. The architectural details of both the classifier and the transfer elements of our model are thoroughly analyzed in this section. The final section presents the results obtained by training these fine-tuned models using tenfold cross-validation. To give a comprehensive view of the models' performance, the mean loss and range of loss for each classifier, as well as for the impact and PLB tests, are plotted. The efficacy of each fine-tuned model is further evaluated by computing and representing key metrics such as precision, recall, and accuracy in a box plot format.

Methods and Experiments

The primary objective of the conducted experiments was to scrutinize the effectiveness of the suggested source localization techniques, utilizing a singular AE sensor, on an aluminum plate. As represented in Figure 1, the experimental setup comprised a sensor, constituted by two frail fiber Bragg gratings (FBGs), forming a low-finesse Fabry-Perot interferometer (FPI) on a coiled single-mode fiber. This arrangement facilitated the detection of ultrasound on a solid surface. The setup employed a narrow-linewidth diode laser with wavelength tunability, designed to direct light toward the FBG-FPI sensor via a circulator developed in Karim et al. (2021).

Before reaching the sensor, the light was passed through a three-paddle polarization controller, which facilitated manual adjustments to the laser polarization. The light reflected from the sensor was then directed to a photodetector (PD) through the same circulator. To obtain acoustic emission signals of higher quality, the output from the PD was amplified and filtered using a 50–500 kHz band-pass filter. Additionally, noise removal techniques, such as adaptive filtering, were employed to reduce any extraneous signals present during data collection. It is selected based on its ability to effectively remove noise while preserving the signal of interest. The filtered and noise-free AE signals were subsequently utilized to train and test the deep learning models for source localization.

Acoustic emission is a physical occurrence linked to stress waves, initiated by the abrupt liberation of elastic energy during the formation of cracks or damages within materials. AE signals can be captured and logged by attaching AE sensors to the sample surface. The AE monitoring process involves the collection and analysis of these signals to assess the condition of the object under study. The Hsu-Nielsen PLB test, a widely accepted artificial method for acoustic emission signal generation (Sause 2011), was used in this study. It involves breaking pencil leads on a surface with an affixed AE sensor. For this study, PLB tests were conducted on a 2.54 mm thick aluminum plate measuring 0.30 × 0.30 m. The plate was partitioned into nine distinct locations as delineated in Figure 2. Each of the nine representative points, denoted by a red dot, underwent the PLB test 10 times, using a 2H mechanical pencil with a 0.5 mm diameter lead.

Furthermore, impact-like signals were gathered by dropping steel balls (4.7 mm diameter) from a height of 25 mm at the same AE sensor location illustrated in Figure 2. The

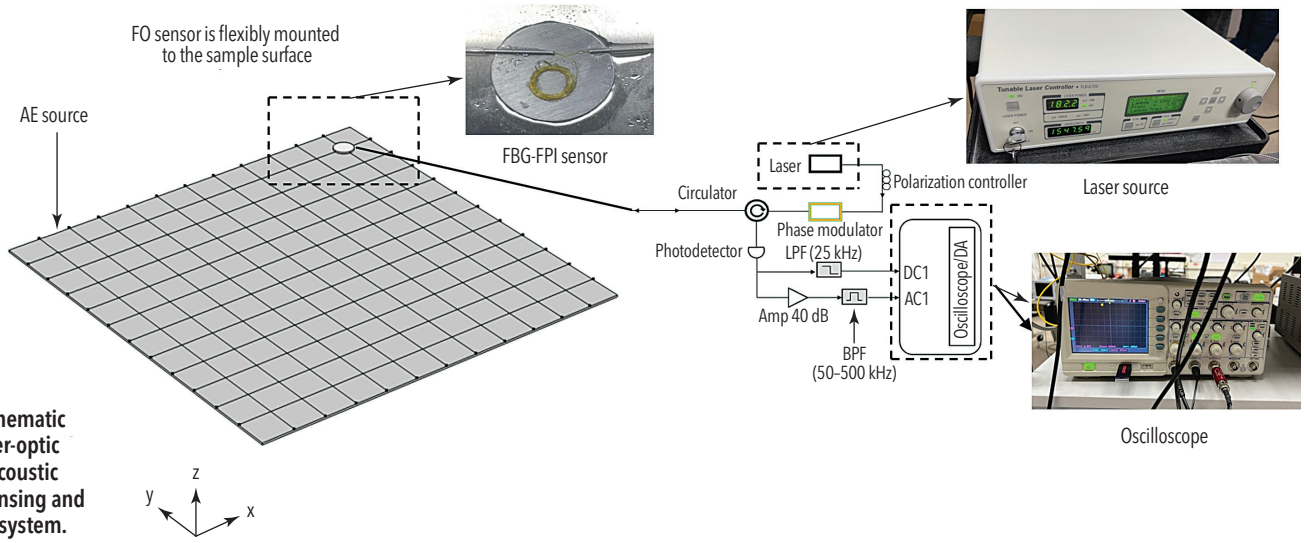

Figure 1. Schematic of novel fiber-optic coil-based acoustic emission sensing and monitoring system.

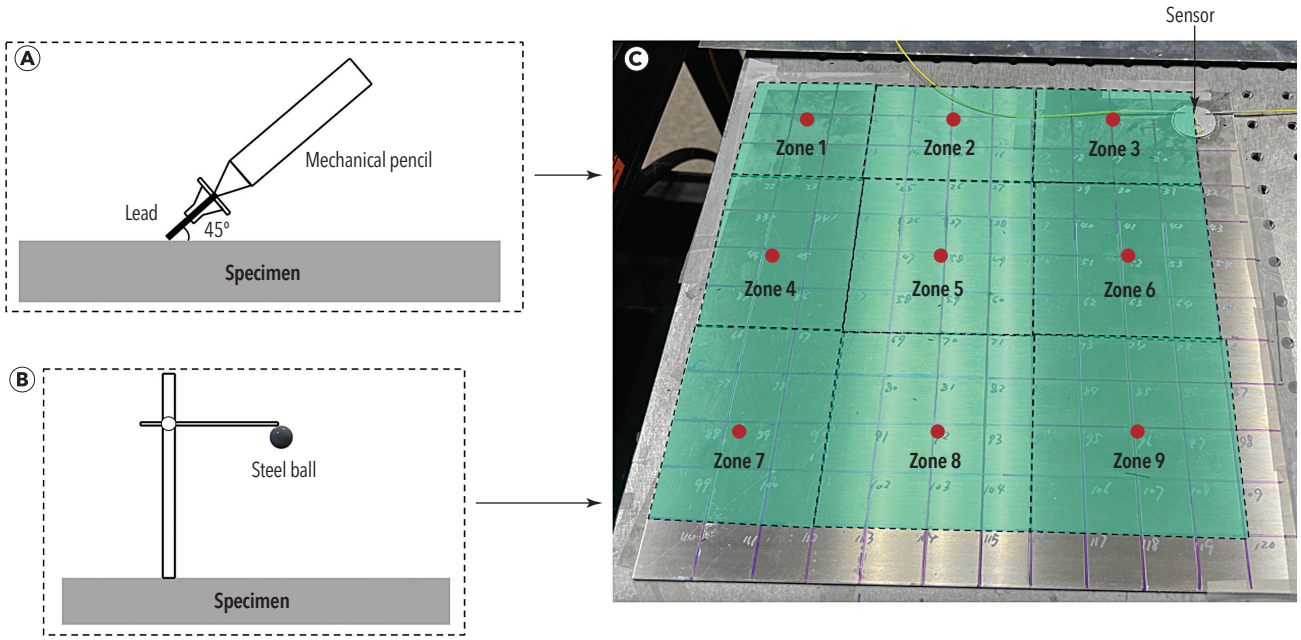

Figure 2. Experimental setup for acoustic emission monitoring: (a) pencil lead break (PLB) and (b) impact tests conducted on an aluminum plate (c) that is segregated into nine identified zones. This setup assists the localization of acoustic emission sources.

equipment and settings for this experiment mirrored those utilized for the PLB tests. The recorded signals were distinguished and examined for acoustic emission source identification and localization, using these procedures. The experimental setup facilitated the collection of precise and accurate data, thereby enabling the evaluation of the proposed method's efficacy in acoustic emission source localization.

Numerical Modeling Assisted Data Augmentation

This study utilizes a 3D computational model for the test specimen to enable an enhanced characterization of acoustic emission impulses, as inspired by Cuadra et al. (2015). The approach hinges on the implementation of pretrained deep learning models, which harness data from FEM-simulated acoustic emission impulses derived from impact-type and PLB tests (Hamstad 2007). The creation of pretraining data via these simulated AE signals propels advancements in acoustic emission source localization within the specimen. This model offers several benefits, such as reducing computational demands and enhancing the performance of AE monitoring systems in real-world scenarios. The accurate characterization of acoustic emission impulses is a vital prerequisite for developing effective signal-processing algorithms. Our proposal presents a robust methodology to pretrain deep learning models using data procured from acoustic emission impulse simulations. The PLB source was strategically positioned in the out-of-plane direction at a predefined location on the plate, with the sensor situated an inch from the right and upper

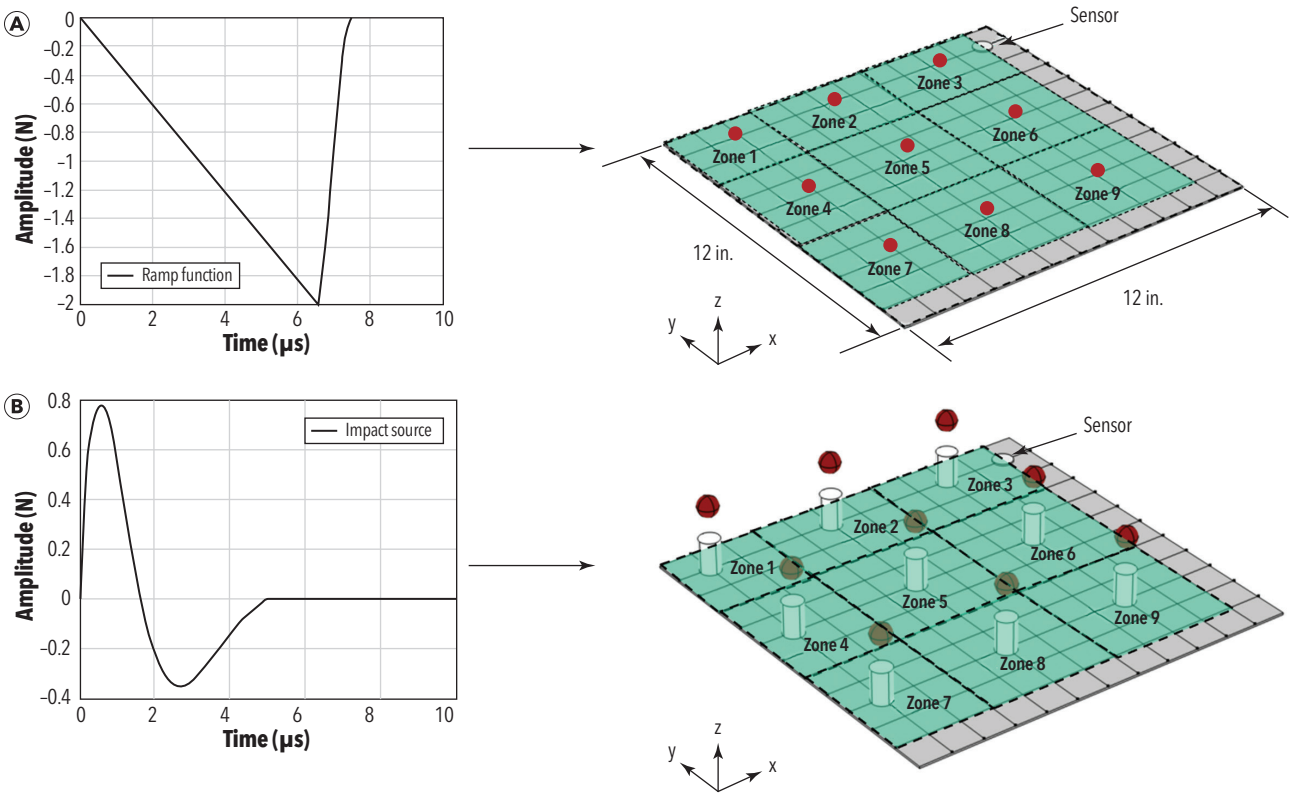

Figure 3. Simulation setup with analytical functions: (a) excitation signal to simulate PLB test; (b) excitation signal to simulate impact test.

edges of the plate, respectively. Utilizing FEM simulations, we generated waveforms from nine distinct locations similar to the experimental setup shown in Figure 2. Simulating AE signals via FEM allows us to generate pretraining data for deep learning models, thereby enabling a more accurate and efficient localization of acoustic emission sources within the specimen. These simulated signals furnish an effective means to pretrain deep learning models for AE signal processing algorithms, consequently bolstering the accuracy and effectiveness of these algorithms in real-world contexts. For the PLB test, the excitation signal, $F_1(t)$, simulates the response of an aluminum plate to mechanical loading and is defined as follows:

$$F_1(t) = \begin{cases} -2t/t_1, & 0 < x < t_1 \\ -cos(\pi[t - t_1]) - 1, & t_1 < x < t_2 \\ 0, & t_2 < x \end{cases}$$

The function was selected due to its ability to elicit a gradual increase in the excitation signal. Here, t_1 and t_2 are time intervals that define specific stages of the excitation signal. t_1 signifies the duration over which the excitation signal increases gradually, while t_2 denotes the time after which the signal ceases. This particular function was chosen as it prompts a gradual increase in the excitation signal, thus adequately representing the mechanical loading process. For the impact test, $F_2(t)$ is represented as:

$$F_2(t) = Ce^{-\gamma t/t_0}\sin\left(\frac{4\pi}{1+\frac{t_0}{t}}\right)$$

where

C is the initial amplitude of the excitation signal,
γ is the damping factor,
t_0 is the characteristic time of the excitation signal, and
t is time.

This function, representing a damped sinusoidal wave, is a common signal observed in impact tests and serves to simulate the material response to mechanical loading. The shape of the

TABLE 1
Parameters for simulation

Parameters	Values
Young's modulus	206 GPa
Poisson's ratio	0.3
Density	2710 kg/m^3
t_0	5 μs
t_1	6.5 μs
t_2	7.5 μs
Decay rate γ	1.85

$F_1(t)$ and $F_2(t)$ is shown in Figure 3 and specifications of these parameters are shown in Table 1.

Figure 4 showcases the signals derived from the impact and PLB tests and their corresponding simulation signals. We present these waveforms to emphasize the clear correlations and dissimilarities between test and simulation data; such contrasts highlight the feasibility of employing deep learning models in acoustic emission source localization. The duration of these signals is distinct for the tests and simulations; the test signals span a duration of 250 µs, while the simulation signals extend over a period of 100 µs. This discrepancy is a consequence of the methods employed to gather sufficient

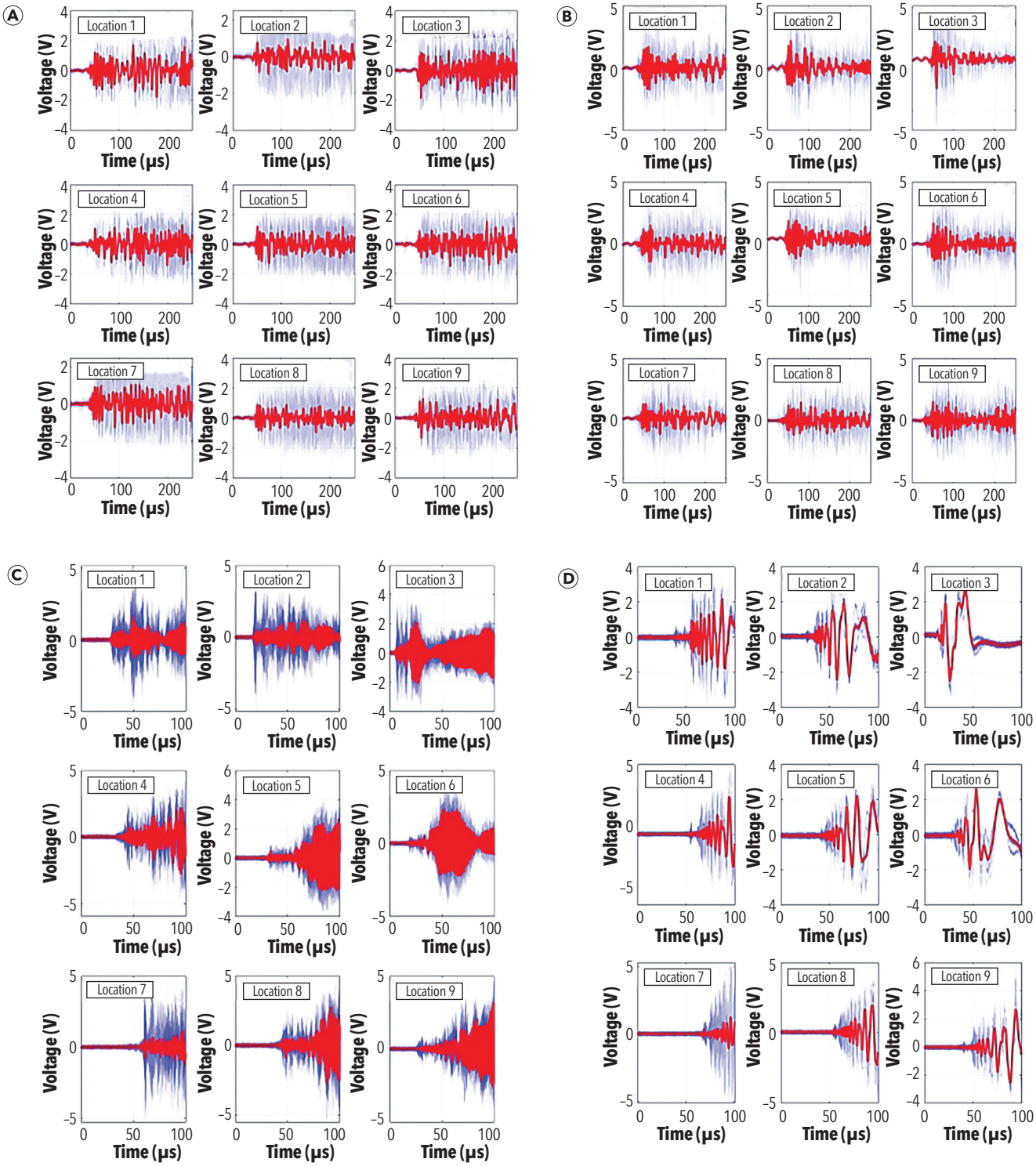

Figure 4. Signals obtained from: (a) impact test; (b) PLB test; (c) impact simulation; and (d) PLB simulation. The raw signal is denoted in blue, while the red line signifies the average waveform.

data from finite element modeling. We deployed a point domain network consisting of a 5×5 grid of sensing locations to gather the simulation data, which increases the complexity of the surrounding mesh, substantially slowing the collection of the reverberation pattern (reflected signals after 100 µs). As such, for practicality and computational efficiency, we limited the simulation data collection to the initial 100 µs. The simulation was conducted using a workstation equipped with a 3.1 GHz multi-core processor and a 4 GB dedicated graphics card. On average, each round consumed approximately 40 min. To gather an adequate volume of source domain data (simulation dataset), a data augmentation process was executed, resulting in the accumulation of 900 waveforms. It is noteworthy that differences in the reflection and trigger mechanisms between simulations and experiments, as observable in the figures, stem from variations in the interaction with adjacent substrates and boundary conditions, resulting in distinct reverberation patterns. Furthermore, while the simulation model logs the accurate time of arrival, the experimental process depends on manual trigger thresholding.

t-SNE is a powerful technique for visualizing high-dimensional data by mapping each data point to a two- or three-dimensional space. While t-SNE was originally designed for static data, it has been adapted for use with time series data in some cases. Visualizing AE data can be challenging due to its complexity and high dimensionality. However, t-SNE can be used to map time series data onto a low-dimensional space while preserving its underlying structure. To apply t-SNE to time series data, we first need to transform the sequential nature of the data into a set of fixed-length feature vectors that can be used as input to t-SNE. This can be done using various techniques such as sliding windows or feature extraction methods like Fourier transforms or wavelet transforms. Once we have transformed the time series data into feature vectors, we can compute pairwise similarities between them using a Gaussian kernel:

$$p_{I_i j} = \frac{\exp\left(\frac{-\|x_i - x_j\|^2}{2\sigma^2}\right)}{\sum_k \sum_l \exp\left(\frac{-\|x_k - x_l\|^2}{2\sigma^2}\right)}$$

where

x_i and x_j are two feature vectors,
sigma is a parameter that controls the width of the Gaussian kernel, and
$p_{I_i j}$ is the probability that x_i would pick x_j as its neighbor if neighbors were picked in proportion to their probability density under a Gaussian centered at x_i.

Next, we compute pairwise similarities between points in the low-dimensional map using a Student-t distribution:

$$q_{i,j} = \frac{\left(1 + \|y_i - y_j\|^2\right)^{-1}}{\sum_k \sum_l \left(1 + \|y_k - y_l\|^2\right)^{-1}}$$

where

y_i and y_j are two points in the low-dimensional map, and
$q_{i,j}$ is the probability that y_i would pick y_j as its neighbor if neighbors were picked uniformly at random from all other points.

Finally, t-SNE minimizes the difference between these two distributions using gradient descent on a cost function that measures their divergence:

$$KL(P\|Q) = \sum_i \sum_j p_{i,j} \log \frac{p_{i,j}}{q_{i,j}}$$

We've employed this t-SNE technique to enhance our understanding of the relationship between our simulation and experimental datasets. Two-dimensional plots generated by this method, as depicted in Figure 5, showing the similarities between AE signals collected from nine distinct zones. Figures 5a and 5b demonstrate that the experimental data from both the impact and PLB tests exhibit larger variability and less distinct clustering, suggesting more complexities and uncertainties in real-world scenarios. On the other hand, Figures 5c and 5d illustrate that the simulation data from both tests have a clearer clustering effect, indicating the advantages of using controlled and predictable simulation data for improving AE source localization techniques. Nevertheless, it's important to recall that the simulation data might not encapsulate all the complexities and variations inherent in real-world scenarios. Therefore, further optimization of our proposed source localization techniques is necessary to incorporate more uncertainty factors, ensuring effectiveness across diverse real-world applications.

Deep Transfer Learning for Knowledge Transfer

This study investigates the effective application of transfer learning to new data, leveraging the insights obtained from pretrained models. A variety of deep learning models, including convolutional neural network (CNN), fully connected neural network (FCNN), Encoder, Residual Network (ResNet), Inception, and Multi-Layer Perceptron (MLP), were assessed for their ability to analyze simulated datasets and to extract underlying features using a layer-wise fine-tuning strategy. The employed methodology entailed signal acquisition from the simulated datasets, followed by data preprocessing, feature extraction via fine-tuned deep learning models, and finally classification based on acoustic emission source location. To scrutinize impact and PLB test simulations, six deep learning models with distinct architectures and capabilities were investigated. This innovative strategy leads to a broader comprehension of the data, permitting the recognition of overlooked patterns and features when using a singular model. Detailed summaries of the architectures used for the networks mentioned are as follows:

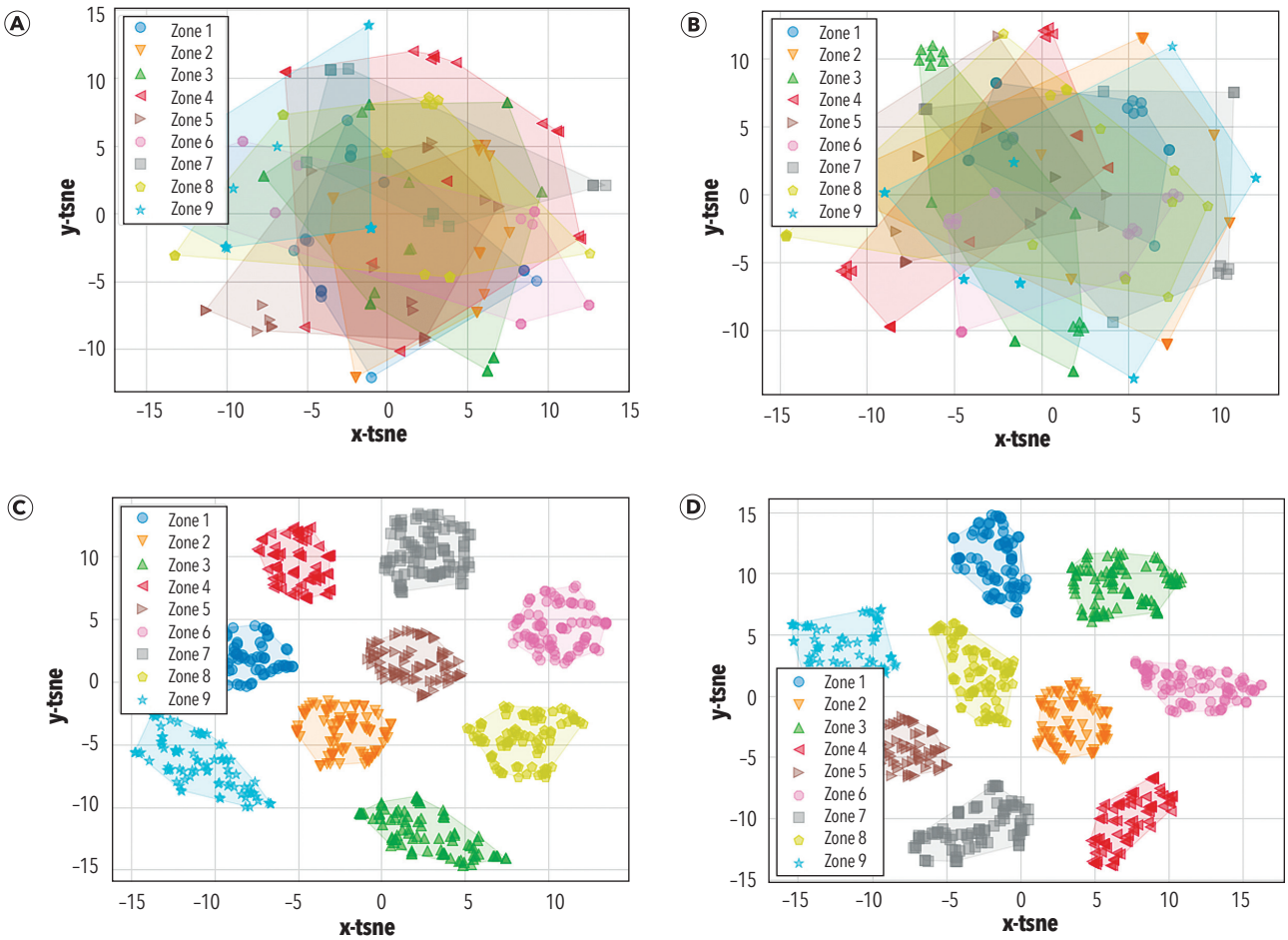

Figure 5. The two-dimensional t-SNE plot for: (a) impact test dataset; (b) PLB test dataset; (c) impact simulation dataset; and (d) PLB simulation dataset.

- CNN implements two convolutional blocks with 1D convolutions, instance normalization, and dropout. Each block comprises a Conv1D layer, succeeded by instance normalization, dropout, and max pooling. Hierarchical features are extracted from the input time series by the convolutional blocks. These features are then flattened and transmitted to a SoftMax classifier. The CNN model employs "categorical_crossentropy" loss and Adam optimizer (Simonyan and Zisserman 2014).
- FCNN resembles the CNN architecture but replaces max pooling with global average pooling to minimize spatial information loss. The global average pooling layer compacts the spatial information into a 1D vector, with these compressed features then passed to the SoftMax classifier (Zhang et al. 2017).
- ResNet uses residual blocks to circumvent the vanishing gradient issue. Residual blocks add the input directly to the stacked convolutional layers, enabling direct gradient flow. It uses batch normalization and weight regularization (L2 regularization). Each residual block comprises two Conv1D layers followed by batch normalization and activation, with the output of the residual blocks average pooled and transmitted to the SoftMax classifier size (He et al. 2015).
- Encoder resembles CNN's convolutional blocks but employs Parametric Rectified Linear Unit (PReLU) activation and instance normalization. After the convolutional blocks, an attention mechanism is applied. This attention layer assigns weights to the feature maps, focusing on pertinent features. The attended features are flattened and passed to the SoftMax classifier extraction (Vincent et al. 2008).
- MLP substitutes the convolutional layers with dense layers for time series classification. The input time series is flattened and sent to the dense layers. It uses two dense layers with dropout for regularization. The output dense layer utilizes SoftMax activation for the classification (Delashmit and Manry 2005).
- Inception utilizes an inception module with parallel branches of 1×1, 3×3, and 5×5 convolutions and max pooling. The outputs of the parallel branches are concatenated, forming the inception module. It employs batch normalization and the dropout post inception module. The features are flattened and transmitted to the SoftMax classifier (Zhang et al. 2022).

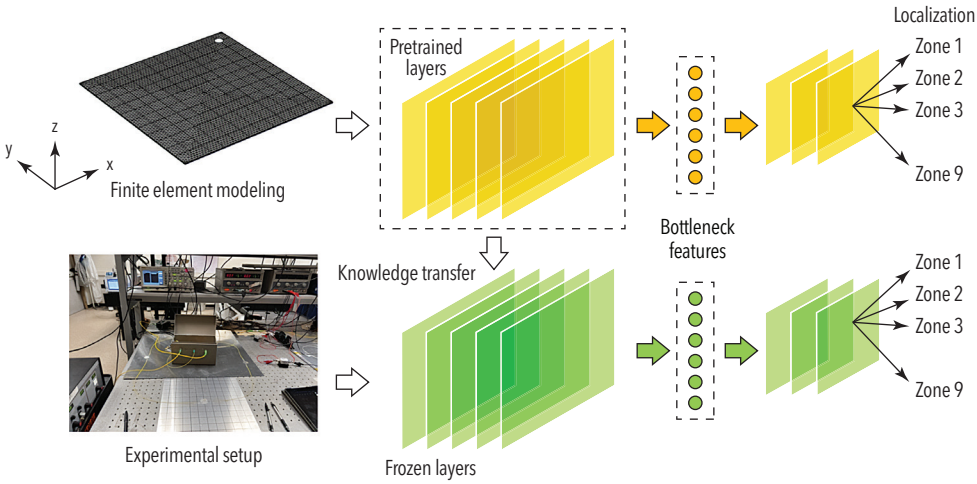

Figure 6. Schematic and structure of knowledge transfer via deep transfer learning.

Our research employs transfer learning, a technique capable of enhancing the performance of deep neural networks across various tasks. We illustrate its efficacy by applying it to improve the performance of deep neural networks in acoustic emission source localization. AE is a nondestructive testing method that leverages sound waves to identify and analyze material defects, and acoustic emission source localization pertains to the determination of the origin of the acoustic emission signals. We initialized our process by pretraining a deep neural network on a large simulation dataset, allowing the network to capture the general features of AE signals. Following this, we fine-tuned the deep neural network on a smaller experimental dataset, a process that facilitated the network's learning of specific features present in the experimental data. Our process involves first transferring layers from a pretrained model, and subsequently freezing their parameters. As new AE data is processed, it passes through these frozen layers before progressing through the trainable layers, allowing us to localize the acoustic emission source. Owing to the intrinsic connection between simulation and experimental data, the feature extractor can be applied to the latter, incorporating it as a nonadjustable layer in our model. We designate the high-level features extracted from these layers as "bottleneck" features due to their high level of condensation and their position at the classifiers' preceding constriction point (as illustrated in Figure 6). The applied deep learning architecture comprises one of six classifiers, each consisting of multiple fully connected layers following global pooling. This design enables nonlinear mapping of bottleneck features to AE source localization. Additionally, a fusion layer is utilized to amalgamate extracted features, and an extra layer is employed to link bottleneck features to location predictions. During fine-tuning, the pretrained model's weights serve as the initial values, and the model undergoes further training with available target domain data. As a consequence, the fine-tuned model can acclimatize to the target domain's unique characteristics, offering superior performance to a model trained from scratch.

Results and Discussion

In this section, we compare the performance of various deep learning models with and without transfer learning applied to acoustic emission source localization tasks. We analyze the mean loss and loss range over 200 epochs for CNN, FCNN, Encoder, ResNet, MLP, and Inception architectures. These models were trained on two different datasets, namely the impact dataset and the PLB dataset, which both contain distinct acoustic emission source localizations. In the first scenario, we trained CNN models without transfer learning directly on the experimental dataset. Both models exhibit a similar pattern over the epochs, initially having high loss values and gradually improving to achieve a significant reduction in loss. However, the validation loss does not decrease as substantially, which may indicate overfitting. In this case, the models have learned the training data too well but struggle to generalize on new, unseen data. In contrast, for the second scenario, we employed transfer learning, where the CNN models were first pretrained on a large, simulated dataset before being fine-tuned on the experimental dataset. Both models begin with lower loss values than those without transfer learning, which could be attributed to the initial learning from the simulated dataset. Over 200 epochs, these models improve significantly. One model achieves a very low validation loss, suggesting excellent generalization capability, while the other model has a slightly higher validation loss. The performance of the other models, such as FCNN, Encoder, MLP, Inception, and ResNet, are also compared with and without transfer learning. Some models, such as the Encoder and MLP, exhibit significant improvements when transfer learning is applied, while others show minor or negligible differences. Interestingly, the ResNet model demonstrates good performance on both the impact and PLB datasets, with and without transfer learning, though it experiences more fluctuations in the loss curve without transfer learning. Figures 7, 8, and 9 illustrate the mean loss and loss range for each model with and without transfer learning on the impact and PLB datasets. These visualizations provide a clear comparison of the models' performances, highlighting the advantages of transfer learning in various cases. In

summary, our findings suggest that transfer learning can significantly enhance the performance of deep neural networks on acoustic emission source localization tasks, particularly when high-quality training data is scarce. It highlights the utility of leveraging preexisting knowledge to expedite learning and bolster the model's ability to generalize. However, not all models benefited from transfer learning. The Inception model's performance was affected slightly, possibly due to the complexities inherent in its architecture. Intriguingly, the FCNN model performed better without transfer learning, indicating that its architecture might be more suited to direct learning from the training data. This observation underscores the need to consider the specificities of each model when applying transfer learning.

The presented study evaluates the performance on the test dataset. Our discussion is supplemented with statistical

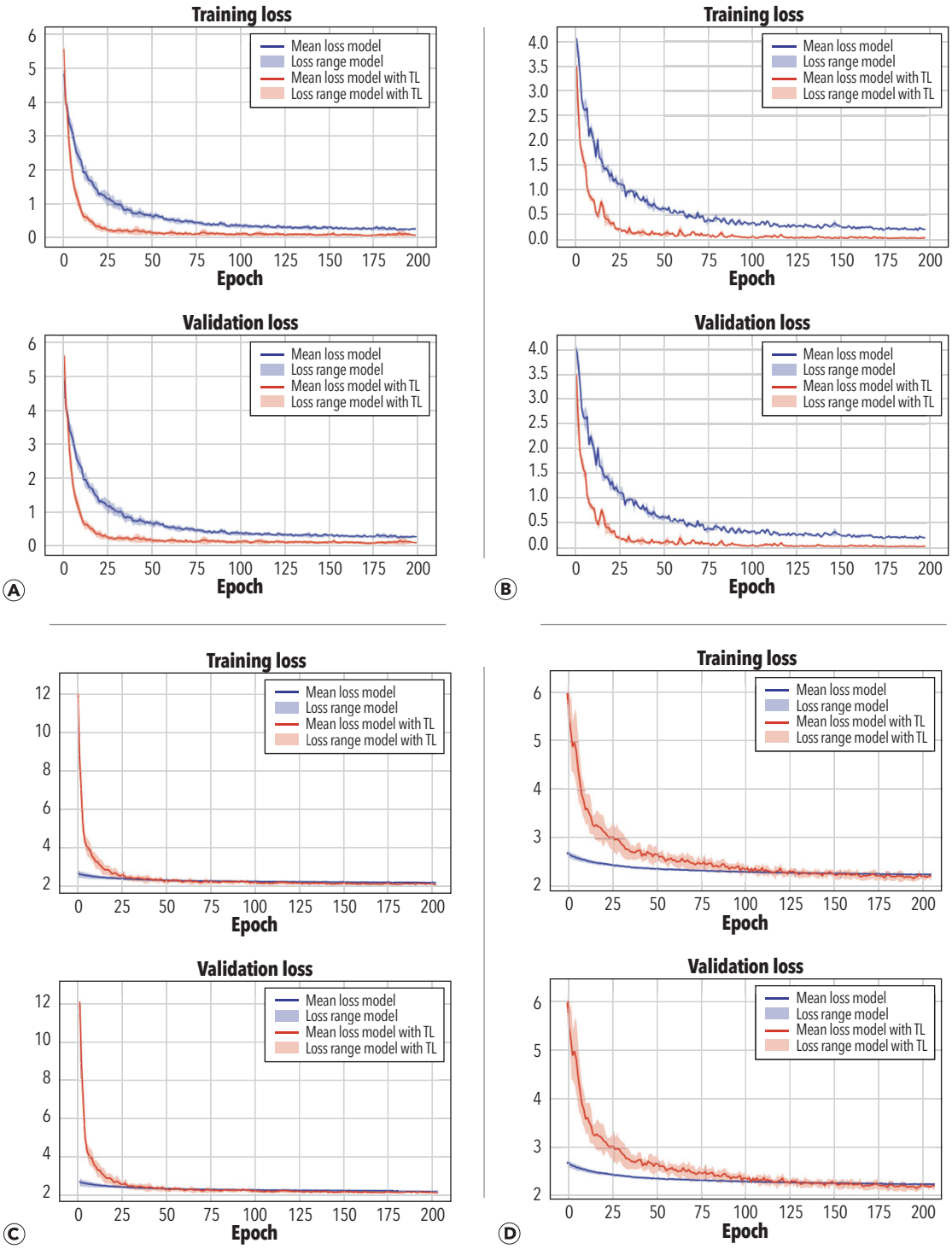

Figure 7. Comparative analysis of mean loss and range with and without the implementation of transfer learning for: (a) CNN model applied to the impact test dataset; (b) CNN model applied to the PLB test dataset; (c) FCNN model applied to the impact test dataset; and (d) FCNN model applied to the PLB test dataset.

metrics such as the minimum (the smallest value in the dataset), maximum (the largest value), median (the middle value when arranged in increasing order), first quartile (Q1: the middle value between the minimum and the median), and third quartile (Q3: the middle value between the median and the maximum). Analyzing the box plot as illustrated in Figures 10 and 11, we have added a few things to reduce overfitting:

- Early stopping: By stopping training if validation loss does not improve for 20 epochs, we prevent the model from overfitting to the training data. If the validation loss is no longer improving, continued training is unlikely to generalize better to new data.
- Restore best weights: By restoring weights from the epoch with the best validation loss, we "roll back" the model to the point before overfitting started to occur. This gives us the model that generalizes best to new data.

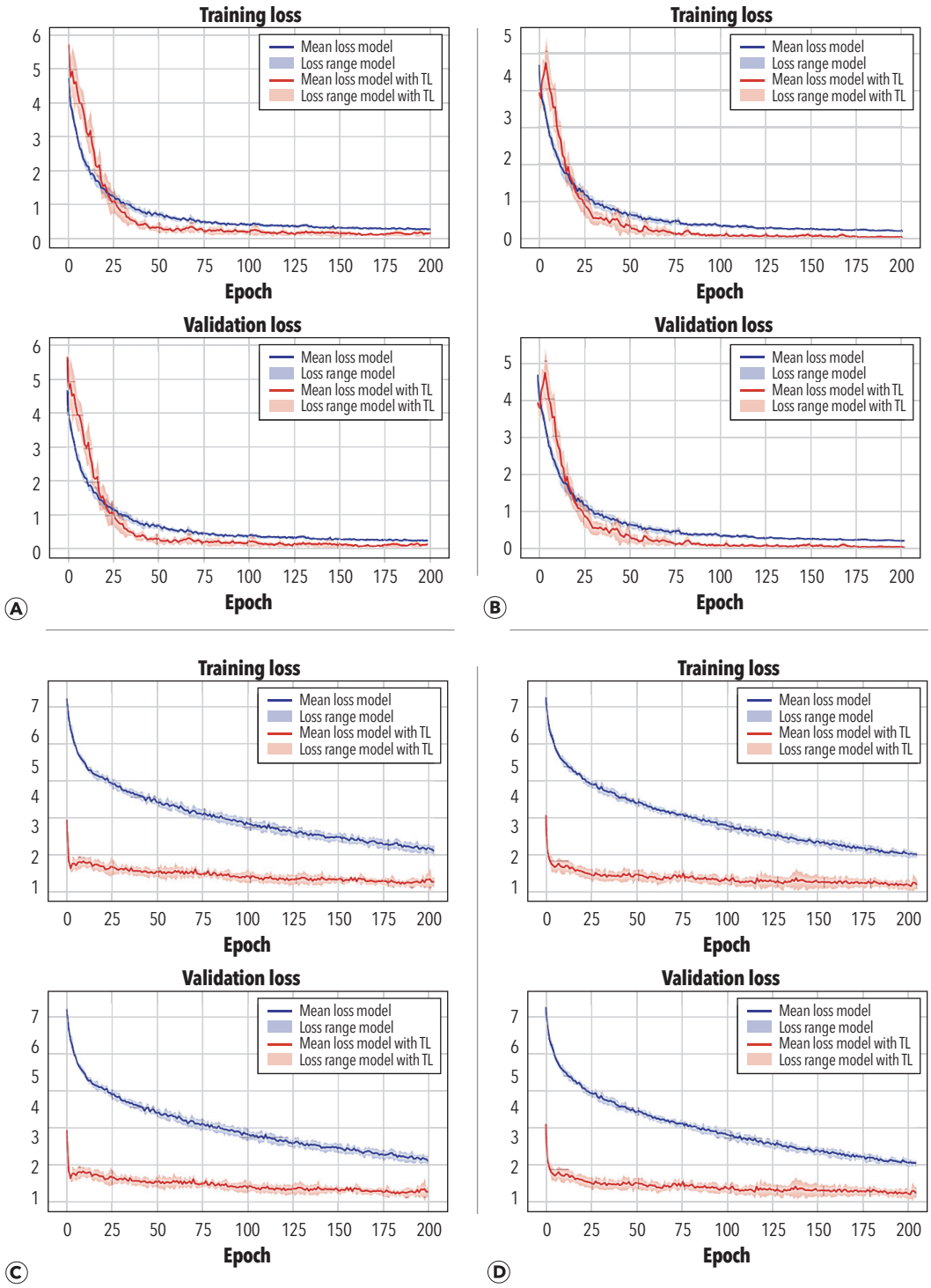

Figure 8. Comparative analysis of mean loss and range with and without the implementation of transfer learning for: (a) Encoder model applied to the impact test dataset; (b) Encoder model applied to the PLB test dataset; (c) MLP model applied to the impact test dataset; and (d) MLP model applied to the PLB test dataset.

- Patience: The patience value of 20 epochs means we are willing to tolerate a fair number of epochs without improvement before stopping training. This avoids stopping too early and allows temporary plateaus in validation loss, but ultimately stops before severe overfitting occurs.

In the Impact dataset, the CNN and MLP models, with and without transfer learning, achieved comparative performance in terms of accuracy, precision, and recall, with slight enhancements observed in models using transfer learning. Conversely, FCNN underperformed, showing negligible improvement from transfer learning; unlike CNN and MLP, which recorded accuracies above 0.8, FCNN yielded a mere 0.2. Transfer learning substantially increased ResNet's performance variance regarding recall, precision, and accuracy. Inception showed a similar trend to CNN and MLP, where transfer learning resulted in minor enhancements. The Encoder model

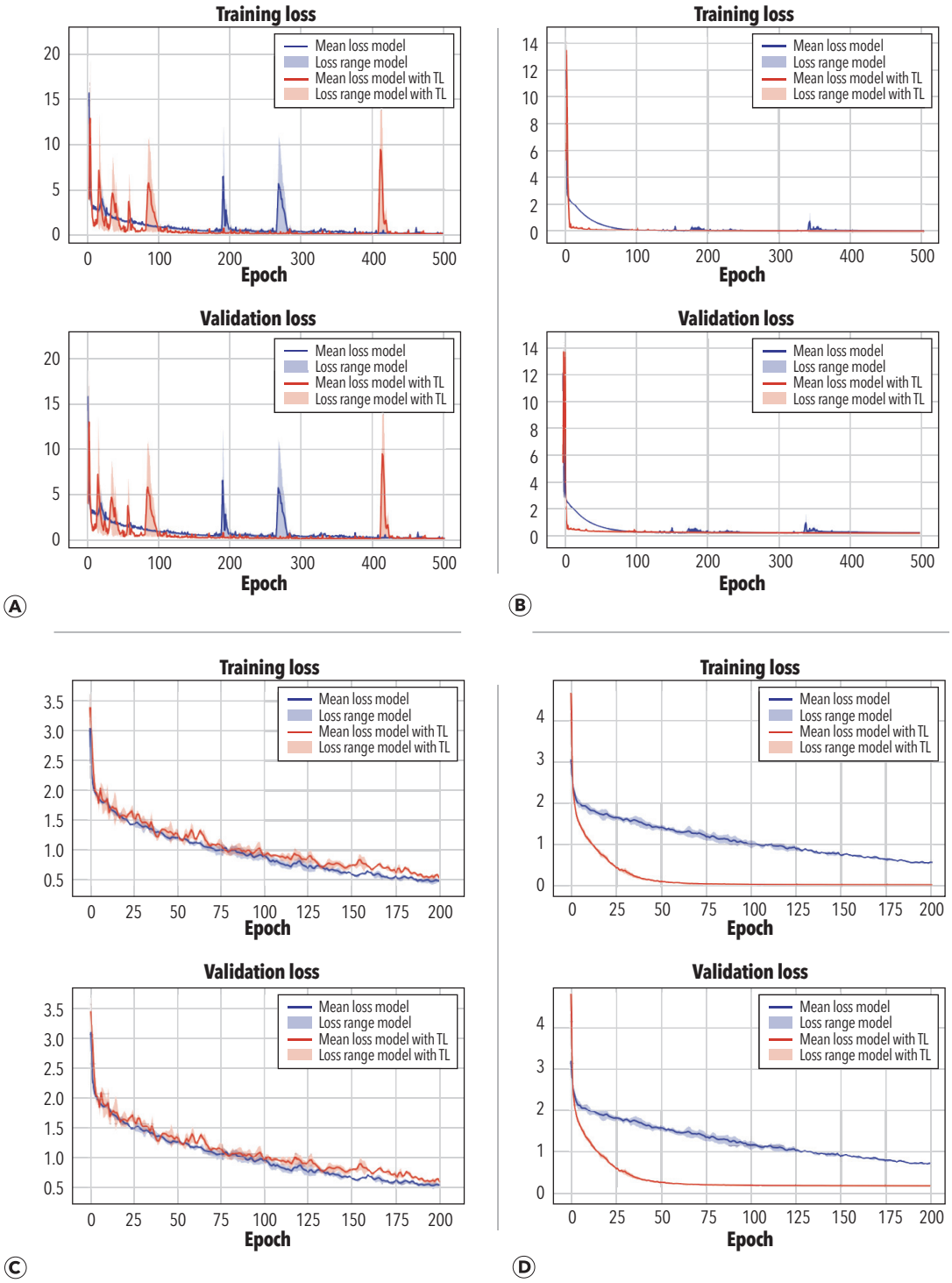

Figure 9. Comparative analysis of mean loss and range with and without the implementation of transfer learning for: (a) Inception model applied to the impact test dataset; (b) Inception model applied to the PLB test dataset; (c) ResNet model applied to the impact test dataset; and (d) ResNet model applied to the PLB test dataset.

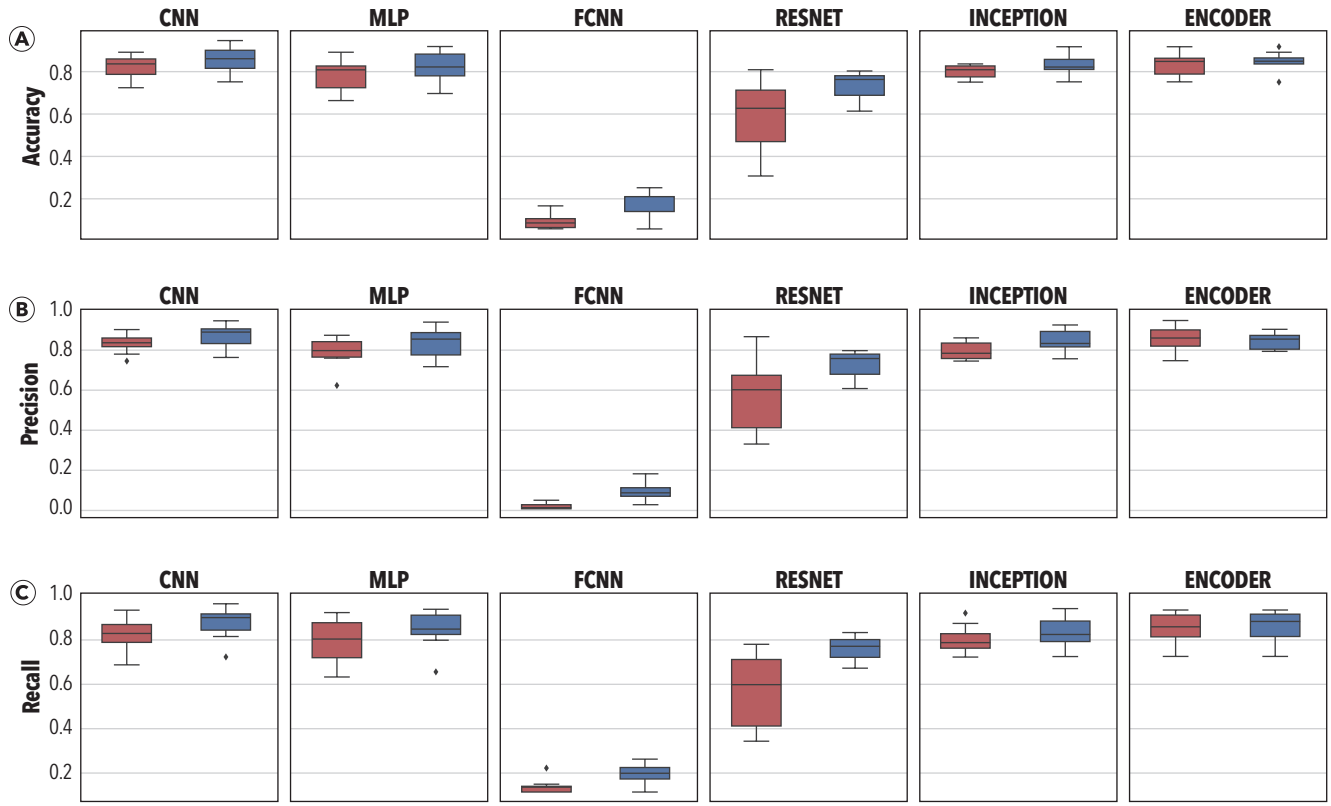

Figure 10. The distribution of: (a) accuracy; (b) precision; and (c) recall from a tenfold cross-validation for six classifiers on the impact test dataset. Models without transfer learning are indicated by red bars, while those with transfer learning are shown in blue.

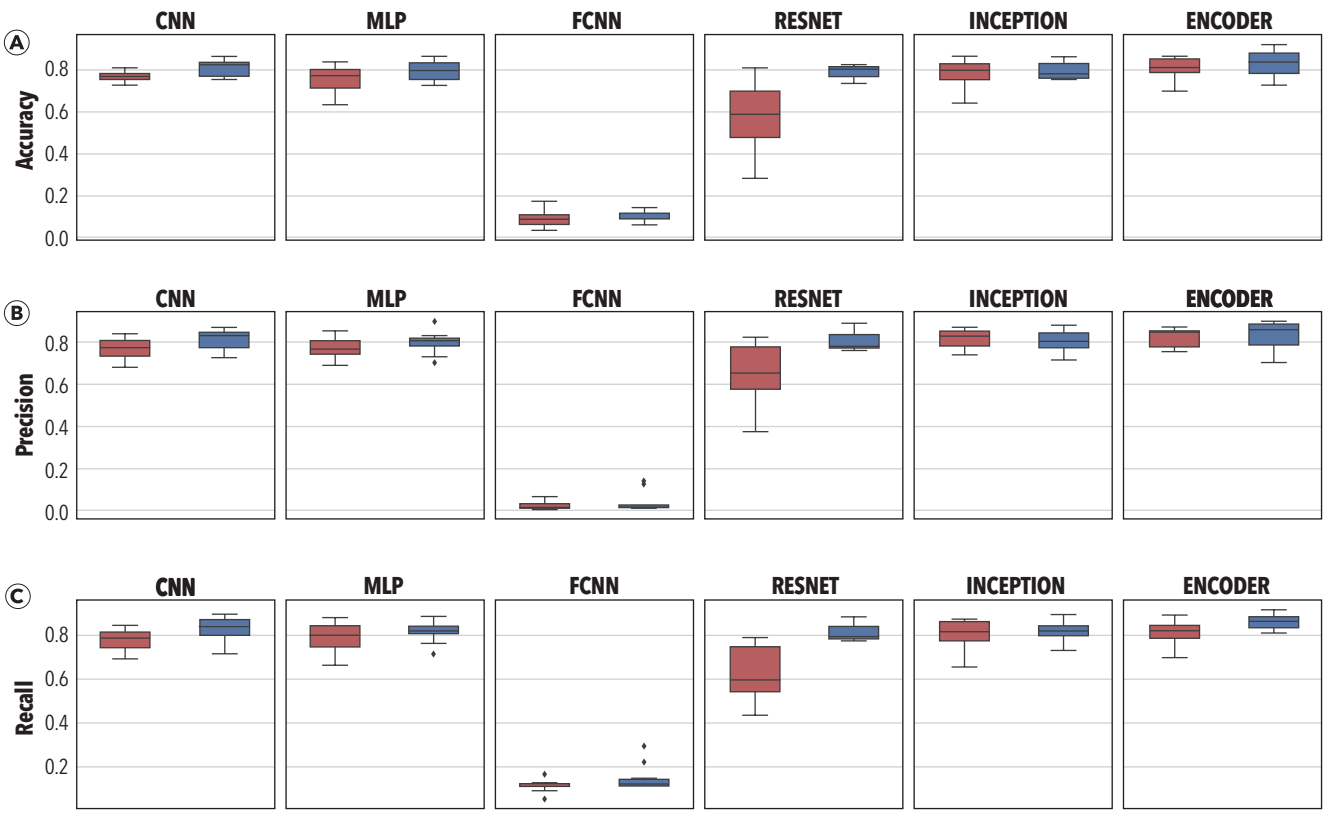

Figure 11. The distribution of: (a) accuracy; (b) precision; and (c) recall from a tenfold cross-validation for six classifiers on the PLB test dataset. Models without transfer learning are indicated by red bars, while those with transfer learning are shown in blue.

showed minimal variation in performance; precision was slightly higher without transfer learning, while recall remained unchanged. Accuracy was slightly improved with transfer learning.

As for the PLB dataset, the CNN and MLP with transfer learning slightly outperformed their counterparts without transfer learning. FCNN underperformed with an accuracy of less than 0.1, while transfer learning further deteriorated its performance. Again, ResNet showed significant improvement through transfer learning. Unlike the Impact dataset, Inception with transfer learning showed slightly worse performance compared to without transfer learning. Encoder, similar to CNN and MLP, had slightly higher precision, recall, and accuracy with transfer learning.

The observations from this study can be explained by the fundamental advantage of transfer learning, which can be explained by the reusability of the learned features. Models without transfer learning, though adept at discriminative patterns from training data, face difficulties in generalizing to unfamiliar data. This process often results in memorizing training data rather than assimilating generalizable patterns, thereby leading to elevated validation losses. On the contrary, models employing transfer learning derive initial benefits from patterns and features harvested from an extensive simulated dataset. These models exhibit reduced initial loss values, indicating that the simulated dataset provides a beneficial starting framework for interpreting the limited experimental data. Furthermore, fine-tuning allowed these models to adapt to the specific characteristics of the experimental data, resulting in significant improvement over epochs and better generalization capabilities. The distinct performance outcomes of different models, as illustrated by statistical metrics and visualizations, underscore the crucial role of model architecture in harnessing the effectiveness of transfer learning.

Conclusions

This paper proposes a novel data-driven approach to accurately localize two types of acoustic emission sources in an aluminum plate using six deep learning models: CNN, MLP, FCNN, Inception, ResNet, and Encoder. The models incorporate deep transfer learning techniques to enhance their effectiveness in identifying the source of acoustic emission signals. The deep learning models were trained and evaluated using simulations of impact and PLB tests with a distributed sensor array designed to maximize information acquisition from the simulations. The results demonstrate the efficacy of deep neural networks with transfer learning in mapping acoustic emission waveforms to their sources and uncovering valuable insights from the simulations. However, this study's limitation is the inability to identify the exact coordinates of the sources of the acoustic emissions. Future research should optimize the deep neural networks using larger training datasets and explore automated solutions like numerical simulations or robotic solutions to address this limitation. Additionally, while in this study Hsu-Nielsen tests were used to simulate fatigue cracks, further research should conduct more formal tests on actual propagating cracks to verify the performance of the proposed deep learning approaches under real states of stress. These efforts could lead to the development of more robust and accurate deep learning models for acoustic emission source localization in real-world applications.

ACKNOWLEDGMENTS

The authors would like to express their gratitude for the research support provided by the US Office of Naval Research under Award No. N00014-20-1-2649 and technical guidance from Program Manager Dr. Ignacio Perez.

REFERENCES

Agarwal, N., A. Sondhi, K. Chopra, and G. Singh. 2021. "Transfer learning: Survey and classification." *Smart Innovations in Communication and Computational Sciences. Advances in Intelligent Systems and Computing*, vol 1168. Springer, Singapore: 145–155. https://doi.org/10.1007/978-981-15-5345-5_13.

Ai, L., V. Soltangharaei, M. Bayat, B. Greer, and P. Ziehl. 2021. "Source localization on large-scale canisters for used nuclear fuel storage using optimal number of acoustic emission sensors." *Nuclear Engineering and Design* 375. https://doi.org/10.1016/j.nucengdes.2021.111097.

Bengio, Y. 2012. "Deep learning of representations for unsupervised and transfer learning." *JMLR: Workshop and Conference Proceedings* 27:17–37.

Chen, S.-X., L. Zhou, Y.-Q. Ni, and X.-Z. Liu. 2021. "An acoustic-homologous transfer learning approach for acoustic emission–based rail condition evaluation." *Structural Health Monitoring* 20 (4): 2161–81. https://doi.org/10.1177/1475921720976941.

Cheng, L., H. Xin, R. M. Groves, and M. Veljkovic. 2021. "Acoustic emission source location using Lamb wave propagation simulation and artificial neural network for I-shaped steel girder." *Construction & Building Materials* 273. https://doi.org/10.1016/j.conbuildmat.2020.121706.

Ciampa, F., and M. Meo. 2010. "Acoustic emission source localization and velocity determination of the fundamental mode A_0 using wavelet analysis and a Newton-based optimization technique." *Smart Materials and Structures* 19 (4): 045027. https://doi.org/10.1088/0964-1726/19/4/045027.

Cuadra, J., P. A. Vanniamparambil, D. Servansky, I. Bartoli, and A. Kontsos. 2015. "Acoustic emission source modeling using a data-driven approach." *Journal of Sound and Vibration* 341:222–36. https://doi.org/10.1016/j.jsv.2014.12.021.

Delashmit, W., and M. Manry. 2005. "Recent developments in multilayer perceptron neural networks." *Proceedings of the 7th Annual Memphis Area Engineering and Science Conference*.

Ebrahimkhanlou, A., and S. Salamone. 2017. "Probabilistic location estimation of acoustic emission sources in isotropic plates with one sensor." *Health Monitoring of Structural and Biological Systems 2017*. 2017. https://doi.org/10.1117/12.2258618.

Ebrahimkhanlou, A., and S. Salamone. 2018. "Single-Sensor Acoustic Emission Source Localization in Plate-Like Structures Using Deep Learning." *Aerospace (Basel, Switzerland)* 5 (2): 50. https://doi.org/10.3390/aerospace5020050.

Ebrahimkhanlou, A., B. Dubuc, and S. Salamone. 2019. "A generalizable deep learning framework for localizing and characterizing acoustic emission sources in riveted metallic panels." *Mechanical Systems and Signal Processing* 130:248–72. https://doi.org/10.1016/j.ymssp.2019.04.050.

Garrett, J. C., H. Mei, and V. Giurgiutiu. 2022. "An Artificial Intelligence Approach to Fatigue Crack Length Estimation from Acoustic Emission Waves in Thin Metallic Plates." *Applied Sciences (Basel, Switzerland)* 12 (3): 1372. https://doi.org/10.3390/app12031372.

Hamstad, M.A. 2007. "Acoustic emission signals generated by monopole (pencil-lead break) versus dipole sources: finite element modeling and experiments." *J. Acoustic Emission* 25.

Hasan, M. J., M. M. M. Islam, and J.-M. Kim. 2019. "Acoustic spectral imaging and transfer learning for reliable bearing fault diagnosis under variable speed conditions." *Measurement* 138:620–31. https://doi.org/10.1016/j.measurement.2019.02.075.

Hassan, F., A. K. B. Mahmood, N. Yahya, A. Saboor, M. Zahid Abbas, Z. Khan, and M. Rimsan. 2021. "State-of-the-Art Review on the Acoustic Emission Source Localization Techniques." *IEEE Access: Practical Innovations, Open Solutions* 9:101246–66. https://doi.org/10.1109/ACCESS.2021.3096930.

He, K., X. Zhang, S. Ren, and J. Sun. 2015. "Deep residual learning for image recognition." Computer Vision and Pattern Recognition. https://doi.org/10.48550/arXiv.1512.03385.

Holford, K. M., A. W. Davies, R. Pullin, and D. C. Carter. 2001. "Damage location in steel bridges by acoustic emission." *Journal of Intelligent Material Systems and Structures* 12 (8): 567–76. https://doi.org/10.1177/10453890122145311.

Ismail Fawaz, H., G. Forestier, J. Weber, L. Idoumghar and P.-A. Muller. 2018. "Transfer learning for time series classification." 2018 IEEE International Conference on Big Data (Big Data), Seattle, WA, USA: 1367–1376, https://doi.org/10.1109/BigData.2018.8621990.

Ismail-Fawaz, A., M. Devanne, J. Weber and G. Forestier. 2022. "Deep learning for time series classification using new hand-crafted convolution filters." *2022 IEEE International Conference on Big Data (Big Data)*: 972–981. https://doi.org/10.1109/BigData55660.2022.10020496.

Karim, F., Y. Zhu, and M. Han. 2021. "Modified phase-generated carrier demodulation of fiber-optic interferometric ultrasound sensors." *Optics Express* 29 (16): 25011. https://doi.org/10.1364/OE.432237.

LeCun, Y., Y. Bengio, and G. Hinton. 2015. "Deep learning." *Nature* 521 (7553): 436–44. https://doi.org/10.1038/nature14539.

Sause, M. G. R. 2011. "Investigation of pencil-lead breaks as acoustic emission sources." *J. Acoustic Emission* 29:184–196.

Simonyan, K., and A. Zisserman. 2014. "Very deep convolutional networks for large-scale image recognition." arXiv preprint. arXiv:1409.1556.

Sun, R.-Y. 2020. "Optimization for deep learning: an overview." *Journal of the Operations Research Society of China* 8: 249–94. https://doi.org/10.1007/s40305-020-00309-6.

Verstrynge, E., G. Lacidogna, F. Accornero, and A. Tomor. 2021. "A review on acoustic emission monitoring for damage detection in masonry structures." *Construction and Building Materials* 268. https://doi.org/10.1016/j.conbuildmat.2020.121089.

Vincent, P., H. Larochelle, and Y. Bengio, P.-A. Manzagol. 2008. "Extracting and composing robust features with denoising autoencoders." *ICML '08: Proceedings of the 25th international conference on machine learning.* https://doi.org/10.1145/1390156.1390294.

Weiss, K., T. M. Khoshgoftaar, and D. Wang. 2016. "A survey of transfer learning." *Journal of Big Data* 3 (1): 9. https://doi.org/10.1186/s40537-016-0043-6.

Zhang, Y., J. Lee, M. Wainwright, and M. I. Jordan. 2017. "On the learnability of fully-connected neural networks." *Proceedings of the 20th International Conference on Artificial Intelligence and Statistics, PMLR* 54:83-91.

Zhang, Y., Y. Hou, K. OuYang, and S. Zhou. 2022. "Multi-scale signed recurrence plot based time series classification using inception architectural networks." *Pattern Recognition* 123. https://doi.org/10.1016/j.patcog.2021.108385.

A MESSAGE FROM YOUR OUTGOING PRESIDENT

DANNY L. KECK
ASNT PRESIDENT, 2022-2023
VICE PRESIDENT, ASNT CERTIFICATION SERVICES LLC
VICE PRESIDENT, ASNT FOUNDATION
DKECK@ASNT.ORG

I would like to take this occasion to say, thank you! It has been an honor and privilege to serve as our Society's 81st President from July 2022 to June 2023. It was a rewarding experience to have the opportunity to work with such a dedicated staff and an extremely professional and effective Board of Directors (BOD) as we together guided our Society through some very trying times. I am so looking forward to taking on the new challenge of serving as Chairperson of the Board beginning in July 2023 as the BOD, including the five new directors just recently elected (see page 88), will continue to strive to make our Society stronger and provide even more opportunities for our members.

Over the past year, we have expanded our portfolio of benefits by acquiring NDT Classroom and we will be further developing those online training courses to fit the needs of our Level I and Level II members (and nonmembers, for that matter). We have successfully administered over 1200+ UT Thickness (UTT) performance verification examinations through our highly successful Industry Sector Qualification (ISQ) performance demonstration program, rolled out the ISQ UT Shear Wave (UT-SW) exams, and are currently rolling out the ISQ UT Phased Array (UT-PA) exams as I write this note in early June. Watch for more on the ISQ program to come in the very near future. Through ASNT Certification Services LLC, a newly formed company that handles all the certification efforts within ASNT, we have finally released the new ASNT 9712 program. This will replace the old ACCP program and will be fully compliant with the latest ISO 9712 standard for the qualification and certification of NDT personnel. Additionally, we have introduced the EBC (employer-based certification) Audit Program wherein service companies can have their in-house SNT-TC-1A and/or CP-189 programs audited by ASNT and receive an accreditation of full compliance for their program once the audit is completed. There is much more to come on this in the very near future that will benefit ASNT members as well.

I was extremely proud to be part of the opening of the new ASNT Houston training and testing facility, as well as the newly formed ASNT India Pvt. Ltd., part of our international expansion efforts. Both of these facilities will provide lower costs to our members while still producing revenue to grow the Society.

During my year-long tenure as President, I was fortunate to have the privilege to represent ASNT at leading NDT conferences around the world. I was asked to attend the British Institute of Non-Destructive Testing (BINDT) annual conference, where I gave a short speech and follow-up toast to their Society. I was honored to host, along with Chairperson of the Board John T. Iman and Vice President Dr. John Z. Chen, the US-Japan NDT Symposium, which is held every four years in Hawaii. I also represented ASNT at the Asia Pacific Conference for NDT in Melbourne, Australia. I was selected and voted in as the President of the next Asia Pacific Conference, which will be hosted by ASNT in Honolulu in 2026. Lastly, I was an invited lecturer at the 70th anniversary ceremonies of the Japanese Society for Non-Destructive Inspection in Tokyo, Japan—an event I will remember for a lifetime. I managed to make a few local section meetings (not as many as I had planned due to unforeseen issues): one being the Charlotte Section's annual shrimp boil, as well as